Geometric interpretation of the γ dose distribution comparison technique: Interpolation-free calculation

Tao Ju[a] and Tim Simpson
Department of Computer Science, Washington University, St. Louis, Missouri 63110

Joseph O. Deasy and Daniel A. Low
Department of Radiation Oncology, Washington University School of Medicine, St. Louis, Missouri 63110

(Received 23 October 2007; revised 14 December 2007; accepted for publication 21 December 2007; published 12 February 2008)

The γ dose comparison tool has been used by numerous investigators to quantitatively compare multidimensional dose distributions. The γ tool requires the specification of dose and distance-to-agreement (DTA) criteria for acceptable variations between the dose distributions. The tool then provides a comparison that simultaneously evaluates the dose difference and distance to agreement of the two dose distributions. One of the weaknesses of the tool is that the comparison requires one of the dose distributions to have a relatively high spatial resolution, with points spaced significantly closer than the DTA criterion. The determination of γ involves an exhaustive search process, so the computation time is significant if an accurate γ is desired. The reason for the need for high spatial resolution lies with the fact that the γ tool measures the closest point in one of the dose distributions (the evaluated distribution) with individual points of the other distribution (the reference distribution) when the two distributions are normalized by the dose difference and DTA criteria for the dose and spatial coordinates, respectively. The closest point in the evaluated distribution to a selected reference distribution point is the value of γ at that reference point. If individual evaluated dose distribution points are compared, the closest point may not accurately reflect the closest value of the evaluated distribution as if it were interpolated on an infinite resolution grid. Therefore, a reinterpretation of the γ distribution as the closest geometric distance between the two distributions is proposed. This is conducted by subdividing the evaluated distribution into simplexes; line segments, triangles, and tetrahedra for one, two, and three-dimensional (3D) dose distributions. The closest distance between any point and these simplexes can be straightforwardly computed using matrix multiplication and inversion without the need of interpolating the original evaluated distribution. While an exhaustive search is still required, not having to interpolate the evaluated distribution avoids the drastic growth of calculation time incurred by interpolation and makes the γ tool more practical and more accurate. In our experiment, the geometric method accurately computes γ distributions between 3D dose distributions on a $200\times200\times50$ grid within two minutes. [DOI: 10.1118/1.2836952]

Key words: radiation therapy, dose distribution comparison, gamma comparison tool

I. INTRODUCTION

Implementation of advanced treatment planning and delivery systems has resulted in the development and use of multidimensional dosimeters. These dosimeters provide the user with large amounts of dose measurement data that need to be analyzed by comparison with either other measurements or calculations. The challenge of the comparisons of planar dose data resulted in the definitions of useful dose comparison tools that have provided the user quantitative evaluations of the differences between the two dose distributions. Some of these analysis tool operators are symmetric with respect to the two dose distributions, but some are not. This is resolved by labeling one of the distributions as a reference and one as the evaluated dose distribution. While these labels imply a specific superiority or unique character of the reference dose distribution relative to the evaluated dose distribution, the user needs to understand the mathematical comparison operators to determine which of the two dose distributions to select as the reference.

The dose comparison tools were reviewed by Low and Dempsey[1] and include the dose-difference tool and the distance-to-agreement (DTA) tool.[2,3] The dose-difference tool computes the numerical dose difference between the two dose distributions at common points. The dose-difference tool tends to be overly sensitive to discrepancies between the two dose distributions in regions of steep dose gradients. The DTA tool is computed for each reference dose point and examines the evaluated dose distribution for the nearest location that has the same dose as the reference point. The DTA tool tends to be overly sensitive in shallow dose gradient regions, where small dose differences can lead to large DTA values. Based on the complementary sensitivity of these two tests, a third tool, termed the composite tool,[2,4] was developed that examines the regions that fail the dose-difference and DTA tests. Unlike the dose-difference and DTA tests, the composite tool requires the user to select acceptance criteria to describe the comparison outcomes. The result is a binary distribution indicating the locations that

failed both the dose-difference and DTA tests. Therefore, the two distributions can be considered equivalent if either (a) the dose differences are within user-specified criteria, or (b) the DTA is within an acceptable distance. A weakness of the composite tool is that it does not provide a continuous scalar comparison value. Therefore, the user does not know by how much the dose distributions passed or failed the test.

To overcome some of the limitations of the composite test, Low *et al.*[1,5] developed a tool called the γ tool. The γ tool provides a comparison distribution consisting of a continuous range of values that characterize the difference between the reference and evaluated distributions relative to user-specified acceptance criteria. Investigators have used the γ tool to compare dose distributions.[6–15] The performance of the γ tool has also been investigated by Caccia *et al.*[7] and Stock *et al.*[16]

Like the DTA tool, implementation of the γ tool requires a search process within the evaluated distribution for each point in the reference distribution. One of the challenges of implementing the γ calculation is that the spacing between points in the evaluated dose distribution is often large when compared against the distance criterion. This leads to artifacts in the γ dose calculation in regions of steep dose gradients. One method of reducing the artifacts is to interpolate the evaluated distribution to a spatial resolution consistent with acceptable interpolation artifacts. This increases the number of points that require interrogation when computing γ and consequently some alternatives to γ have been proposed.

Bakai[17] proposed a modification to the γ tool, whereby an ellipse within the spatial axes was defined around each reference point. Rather than renormalizing both the dose and distance dimensions, the dose dimension was modified by multiplying the dose by the ratio of DTA to dose-difference criteria. The modified dose axis had units of distance, consistent with the spatial axes. The acceptance ellipses used in the γ calculation became a tube (for a one-dimensional example) that followed the reference distribution. The goal of the evaluation was to determine where the evaluated distribution entered the tube and consequently passed the comparison test. In order to make the evaluation process more efficient, Bakai *et al.*[17] used the tube concept to define an evaluation factor χ, which was computed once for each reference point. The acceptance criterion at a reference point was determined using the local dose gradient, the dose-difference and DTA criteria. The value of χ was the ratio of the dose difference to the locally determined acceptance criterion, and if $\chi \leq 1$, the comparison passed. They found that their χ evaluation was 120 times faster than the original γ evaluation. One limitation of the χ evaluation was that it required the evaluated and reference distribution to be on the same grid resolution so that the gradient of the reference distribution could be determined. The original γ algorithm works for any reference distribution spatial density.

Depuydt *et al.*[18] used a filter cascade method for reducing the interpolation artifacts in the γ calculation. Their method produced a pass/fail metric. They limited the evaluation point search to the spatial radius of the DTA criterion. If the closest evaluation dose distribution point was not within the acceptance ellipsoid the evaluation process failed at that reference dose point. An exhaustive search was conducted within the local region of the reference dose point, and as soon as a single reference dose point was found that would pass the γ criteria, the search was ended. If no points within the local region passed, then another search was done to determine if the dose difference changed sign within the local region. If so, there must have been a location (which would require interpolation to locate) where the dose difference was zero, and consequently $\gamma \leq 1$. Finally, if the evaluation failed, a third test was conducted to determine if an evaluation point just outside the DTA distance had an opposite sign of the evaluation points just inside the DTA distance. If so, the γ test was said to pass at the reference dose point. The multistep cascade process resulted in an efficient method of determining whether the two distributions lay within or without the dose-difference and DTA criteria, but provided only a pass/fail result, not the continuous value of γ.

Wendling *et al.*[19] recently reported a method for improving the performance of the γ algorithm. They conducted the exhaustive search for γ by interpolating the evaluated distribution, but conducting the search in a radial pattern, starting at the reference dose point, and precomputing and storing the interpolation factors. They found a better than 75% reduction in calculation time when using this approach. However, the use of uniform interpolation of the evaluated distribution made the calculation time grow cubically with the increase in grid resolution. According to their report, the calculation time typically exhibited an eightfold increase each time the grid spacing was reduced by half through interpolation.

The reason that γ requires significant computer resources is due to the need for interpolation. In the renormalized dose-distance space, the process of determining γ is equivalent to locating the shortest distance that the evaluated dose distribution makes to the reference dose point. For one-dimensional dose distributions, the shortest distance lays at either an evaluated dose point or is normal to lines connecting neighboring evaluated dose points (linear interpolation). By approaching the problem as a geometric one, powerful geometric interpolation algorithms can be applied to the computational challenge.

II. METHODS AND MATERIALS

The formalism for computing γ was published by Low and Dempsey[1] but is repeated here for clarity. The γ function is defined for each reference dose point r_r as

$$\gamma(r_r) = \min_{r_e} \Gamma(r_r, r_e), \tag{1}$$

where r_e refers to the evaluated dose distribution points. The value of Γ is determined for each reference and evaluated dose point pairs as

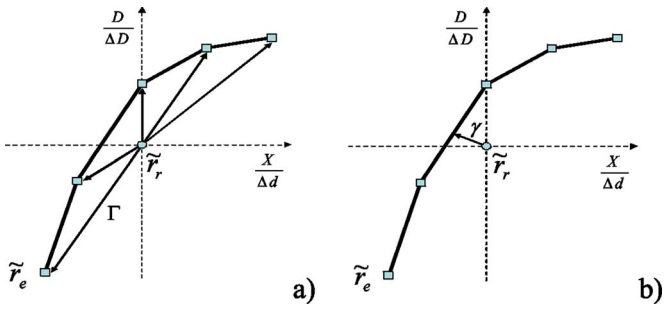

FIG. 1. One-dimensional example: (a) Evaluating Γ by using original evaluated dose points at steep-dose gradients in a one-dimensional distribution. (b) Computing γ as the geometric distance from the normalized reference point $\tilde{r}_r$ to the dose curve representing normalized evaluated distribution.

$$\Gamma(r_r,r_e)=\sqrt{\frac{|r_e-r_r|^2}{\Delta d^2}+\frac{[D_e(r_e)-D_r(r_r)]^2}{\Delta D^2}}, \tag{2}$$

where D_r and D_e are the reference and evaluated dose levels, respectively, and Δd and ΔD are the distance-to-agreement and dose-difference criteria, respectively. For the tests presented here, we used $\Delta d=3$ mm and $\Delta D=3\%$.

The quantity γ can be understood from a geometric perspective. In order to do this, renormalize the dose and distance spaces by the criteria such that the reference and evaluated points become $\tilde{r}_r=(r_r/\Delta d, D_r(r_r)/\Delta D)$ and $\tilde{r}_e=(r_e/\Delta d, D_e(r_e)/\Delta D)$, respectively. The Γ function in Eq. (2) then becomes the Euclidean distance

$$\Gamma(r_r,r_e)=|\tilde{r}_r-\tilde{r}_e|. \tag{3}$$

In this nomenclature, γ is simply the shortest distance from a normalized reference point $\tilde{r}_r$ to *any* evaluated dose distribution point $\tilde{r}_e$.

II.A. Computing the γ function: The interpolation method

One problem with conducting the γ calculation using the original evaluated dose distribution points, without interpolation, is that the errors of γ in steep dose gradient regions cause artifacts in the resulting γ distributions. The cause of these dose errors is illustrated in one dimension in Fig. 1(a). In this example, the γ evaluation is being conducted in a steep dose gradient region. The minimum distance between a normalized reference point $\tilde{r}_r$ and the set of normalized evaluated pixels can be much larger than the actual distance from $\tilde{r}_r$ to the curve formed by connecting the points $\tilde{r}_e$. The conventional solution to this problem is to linearly interpolate the evaluated distribution at finer grid resolutions, which effectively adds more points with shorter intervals on the curve connecting the original points $\tilde{r}_e$. The interpolation method in current use does reduce the error in γ but also greatly increases the calculation time due to the increase in the number of points to be compared. In addition, the evaluation of Γ at discrete, higher density points, does not eliminate the artifacts, even at high interpolation resolutions.

II.B. Computing the γ function: The geometric method

The γ function measures the shortest distance from a normalized reference point $\tilde{r}_r$ to the evaluated distribution described by the set of normalized evaluated points $\tilde{r}_e$. Instead of interpolating the evaluated distribution at discrete locations, consider the continuous surface that consists of all possible interpolated points, referred to as the *dose surface*. The problem then is to find the closest distance from $\tilde{r}_r$ to this surface. An example of the one-dimensional case is shown in Fig. 1(b). The evaluated dose distribution is a set of points lying in the two-dimensional normalized dose-distance space. The closest distance from $\tilde{r}_r$ to the evaluated distribution, now defined as line segments connecting the normalized evaluated points $\tilde{r}_e$, is γ. Note that this is implicitly applying linear interpolation in the sense that the regions between successive evaluated points are defined by line segments, as opposed to curved segments such as a spline that corresponds to higher order interpolation.

Similarly, for a two-dimensional dose distribution represented as a rectangular array of pixels, the dose surface lies in the three-dimensional dose-distance space and consists of evaluated points connected by quadrilateral elements arranged in a rectangular array. Finally, for a three-dimensional dose distribution, the dose surface is a hyper surface lying in the four-dimensional dose-distance space and consisting of cubical elements.

The problem of efficiently finding the closest distance of a surface to a point has been solved for simplicial meshes. A simplicial mesh is a collection of simplexes, which themselves are surface elements defined by the smallest number of vertices required by the dimensionality of the simplex. Formally, in n-dimensional space, a k-simplex S $(0\leq k\leq n)$ is the convex hull of $k+1$ points (called the vertices of S). For example, possible simplexes in a three-dimensional space are the 0 simplex (a point), the 1 simplex (a line segment), the 2 simplex (a triangle), and the 3 simplex (a tetrahedron), consisting of 1, 2, 3 and 4 vertices. The advantage of working with simplexes over general shapes, such as squares or cubes, is that the distance from a point to a simplex can be computed easily in closed forms (to be discussed next).

The dose surface will be described as a simplicial mesh, which is a collection of simplexes. Given an n-dimensional dose distribution, the dose surface lies in an $(n+1)$-dimensional space, and the simplex dimensionality required to describe the dose surface is $k=n$. For two-dimensional dose distributions $(n=2)$, the three-dimensional dose surfaces are converted to triangular meshes by dividing each square defined by adjacent evaluated dose points into two triangles (the 2 simplex). For three-dimensional dose distributions $(n=3)$, the four-dimensional hyper dose surfaces are converted into tetrahedral meshes by dividing each cube into five tetrahedrons (the 3 simplex), as shown in Fig. 2. If the dose surface representing the evaluated dose distri-

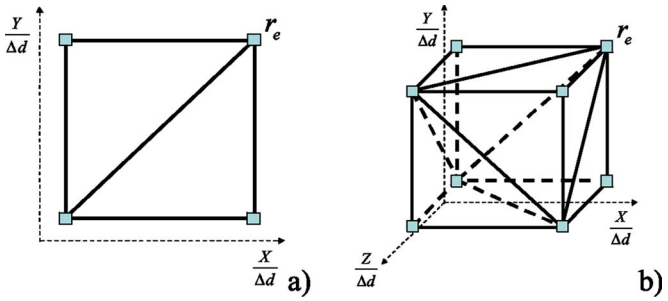

FIG. 2. Subdividing the dose surface into simplexes: (a) For a two-dimensional does distribution, we split each square formed by four pixels into two triangles. (b) For a three-dimensional dose distribution, we split each cube formed by eight voxels into five tetrahedra.

bution is denoted as G_e, and the Euclidean distance from a point p to a simplex S as $D(p,S)$, the function γ is computed geometrically as

$$\gamma(r_r) = \min_{S \in G_e} D(\tilde{r}_r, S). \tag{4}$$

II.C. Computing distance to simplexes

The distance from a point p to a shape S is the shortest distance between p and any point lying on the boundary or in the interior of S. To compute this distance, we first observe that any boundary or interior point v of a *convex* shape S (which simplexes are) can be expressed as

$$v = \sum_{i=1}^{k+1} w_i v_i \tag{5}$$

where $\{v_1, \ldots, v_{k+1}\}$ are vertices of S, and $\{w_1, \ldots, w_{k+1}\}$ is a set of non-negative weights that are partitions of unity, e.g., $\Sigma_{i=1}^{k+1} w_i = 1$. Equation (5) can be used to compute the individual components of v (e.g., x, y, and z). In addition, when S is a simplex and the weights w_i are allowed to assume negative values, Eq. (5) yields points that form the *support* of S. Intuitively, the support of a k simplex is a line ($k=1$), a plane ($k=2$), or a hyper-plane ($k=3$) that contains that simplex. As an example, in the case of $k=2$, Eq. (5) implies that every point on the two-dimensional plane containing a triangle S can be expressed as a weighted combination of the three vertices of that triangle.

To compute the distance from a point p to a k-simplex S ($k>0$), first consider the distance from p to the support of S, which can be expressed as the minima

$$\bar{D}(p,S) = \min_{\{w_1,\ldots,w_{k+1}\}, s.t. \sum_{i=1}^{k+1} w_i = 1} \left| p - \sum_{i=1}^{k+1} w_i v_i \right|. \tag{6}$$

Because any point v on the support (either inside or outside S) can be defined by a sum $\Sigma_{i=1}^{k+1} w_i v_i$, the right-hand side of Eq. (6) simply denotes the shortest distance between the point p and any point v on the support. In the case of $k=2$ (i.e., S is a triangle), the shortest distance $\bar{D}(p,S)$ is described by the line passing through p and normal to the plane containing S. The mathematically powerful feature of Eq. (6) is that it can be formulated as a quadratic minimization problem, whose minimum is achieved when

$$\{w_1, \ldots, w_k\} = (V^T V)^{-1} V^T P, \quad w_{k+1} = 1 - \sum_{i=1}^{k} w_i, \tag{7}$$

where P and V are $n \times 1$ and $n \times k$ matrices, respectively, of the form

$$P = \begin{Bmatrix} c_1(p) - c_1(v_{k+1}) \\ \vdots \\ c_n(p) - c_n(v_{k+1}) \end{Bmatrix},$$
$$V = \begin{Bmatrix} c_1(v_1) - c_1(v_{k+1}) & \cdots & c_1(v_k) - c_1(v_{k+1}) \\ \vdots & \vdots & \vdots \\ c_n(v_1) - c_n(v_{k+1}) & \cdots & c_n(v_k) - c_n(v_{k+1}) \end{Bmatrix}. \tag{8}$$

Here, $c_j(q)$ denotes the jth coordinate of point q for $j = 1, \ldots n$. Note that the inverse $(V^T V)^{-1}$ exists when the simplex S is non-degenerate.

The distance $\bar{D}(p,S)$ computed in Eq. (6) may not be the actual distance from p to the simplex S itself. For example, in the case of $k=2$ (where S is a triangle), the shortest distance between p and the plane containing S refers to a line that passes through p and lies normal to the plane. The intersection of the line with the plane may, or may not lie interior to the triangle S. If the intersection lies outside S, $\bar{D}(p,S)$ is no longer the distance from p to S. The scenario can be detected by checking if one or more of the values of the weights $\{w_1, \ldots, w_{k+1}\}$ computed by Eq. (7) are negative. In these cases, the distance from p to S is the shortest distance between p and the *boundary* of S, denoted as ∂S. In the example where S is a triangle, if one of the weights $\{w_1, \ldots, w_3\}$ is negative, the point on the triangle S that is closest to p lies on the boundary of S, which consists of three line segments.

Interestingly, for a k-simplex S, its boundary ∂S is a collection of $(k-1)$ simplexes. For example, the boundary of a tetrahedron in the dose surface of a three-dimensional dose distribution consists of four triangles, the boundary of a triangle in the dose surface of a two-dimensional dose distribution consists of line segments, and the boundary of a line segment consists of points. This allows the actual distance from p to a k-simplex S to be computed recursively as

$$D(p,S)=\begin{cases}\bar{D}(p,S) & \text{If } w_i \text{ in Eq. (7) are all non-negative}\\ \min\limits_{S_i\in\partial S} D(p,S_i) & \text{Otherwise}\end{cases}. \tag{9}$$

The recursion terminates when S is a 0 simplex (a single point) $\{v_1\}$, where $D(p,S)=|p-v_1|$.

II.D. Fast implementation

The geometric method computes the γ value at each reference dose point by performing an exhaustive search over all nearby simplexes in the dose surface representing the evaluated distribution, as in Eq. (4), and for each simplex, performing a recursive evaluation for the geometric distance, as in Eq. (9). Two strategies are adopted in our implementation to respectively speed up the search and the evaluation process.

First, the simplexes in the evaluated dose surface are sorted by their shortest distances in the dose plane to the reference dose point where γ is to be computed. The radial sorting has been shown to be able to dramatically speed up the exhaustive search.[19] The intuition is that the point on an $(n+1)$-dimensional dose surface representing the evaluated distribution that is closest to the reference dose point is more likely to be located near the reference point in the original n-dimensional dose space. Specifically, we consider an approximate distance from a normalized reference point $\tilde{r}_r=(r_r/\Delta d, D_r(r_r)/\Delta D)$ to a simplex S whose vertices are normalized evaluated dose points $\tilde{r}_e=(r_e/\Delta d, D_e(r_e)/\Delta D)$

$$d(\tilde{r}_r,S)=\min_{\tilde{r}_e\in S}\frac{|r_e-r_r|}{\Delta d}. \tag{10}$$

This approximate distance is the shortest distance from the simplex to the reference point in the original n-dimensional dose space. In the case of two-dimensional dose distributions, $d(\tilde{r}_r,S)$ is the shortest distance on the two-dimensional dose plane between the reference dose point and three evaluated dose points, scaled by the distance-to-agreement criterion. Note that $d(\tilde{r}_r,S)$ is a lower bound of the actual geometric distance $D(\tilde{r}_r,S)$ in the $(n+1)$-dimensional dose-distance space. Utilizing this fact, our program sorts all simplexes S in the ascending order of $d(\tilde{r}_r,S)$, computes the true geometric distance $D(\tilde{r}_r,S)$ for each simplex in this order, and terminates the computation when $d(\tilde{r}_r,S)$ exceeds the minimum geometric distance that has been found so far. This minimum is then the γ value at $\tilde{r}_r$. In practice, the sorting significantly reduces the number of simplexes where the true geometric distance has to be computed compared to an otherwise brute-force search. Note that the sorting can be done as a one-time preprocess [because $d(\tilde{r}_r,S)$ is independent of the actual dose value at r_r] and used for computing γ at all reference points.

Second, the recursion in Eq. (9) can be limited to a subset of all simplexes on the boundary ∂S based on the signs of the weights w_i obtained in Eq. (7). In particular, a boundary simplex only needs to be considered in the recursion if it is opposite to a vertex v_i in S whose associated weight w_i is negative. In the case where S is a triangle (i.e., a 2 simplex), its boundary consists of three line segments (which are 1 simplexes), each opposite to a triangle vertex. Only those line segments whose opposite vertex has a negative weight need to be considered in the recursive evaluation in Eq. (9).

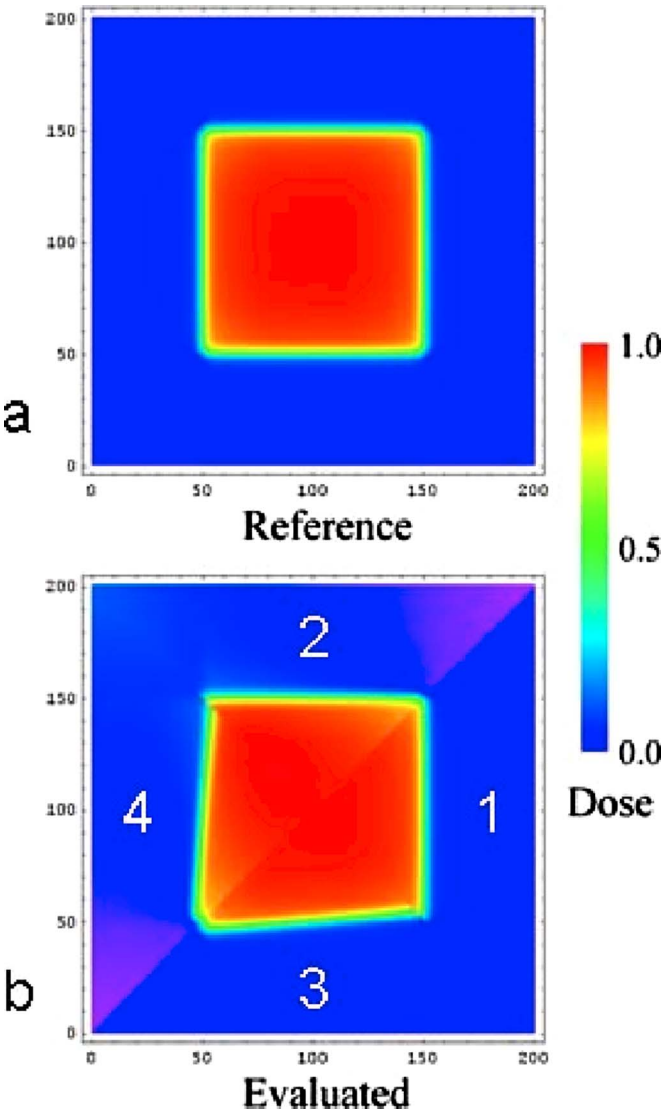

FIG. 3. Two-dimensional reference and evaluated dose distributions used to test the proposed γ calculation algorithm.

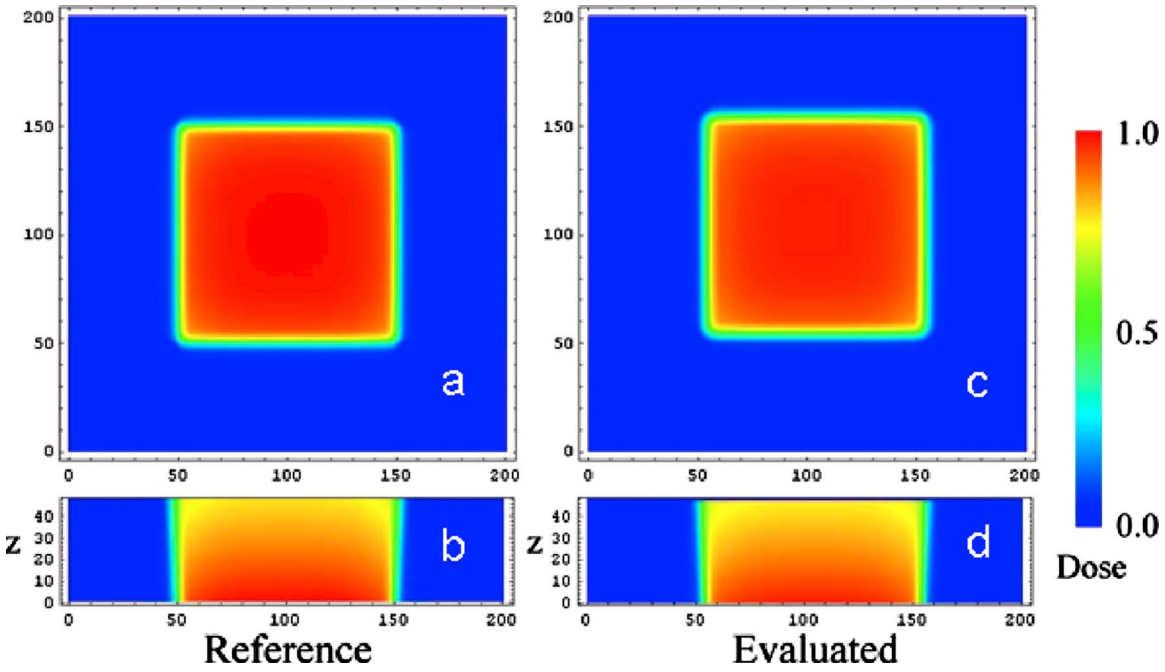

FIG. 4. Three-dimensional reference and evaluated dose distributions used to test the proposed γ calculation algorithm.

II.E. Examples

To evaluate the performance of the geometric computation of γ, the two-dimensional dose distribution simulations that were described in Low *et al.*[1] were employed (Fig. 3). These dose distributions simulated a coronal projection through a 10×10 cm^2, 6 MV photon beam incident on a water phantom. The reference dose distribution was normalized to 1.0 at the central axis, had a maximum dose gradient of 12% mm^{-1}, and had a pixel spacing of 1×1 mm^2. The evaluated distribution was a modified version of the reference designed to highlight the behavior of γ under dose and spatial distortions. The square reference field was divided along the diagonals into four quadrants. Quadrant 1 (right quadrant) was identical to the reference dose distribution. Quadrant 2 (upper quadrant) used the reference dose distribution scaled by a factor proportional to the off-axis distance. The proportionality constant was 1.2% cm^{-1} such that at 2.5 cm off-axis distance, the dose discrepancy was ±3%. Quadrant 3 (lower quadrant) used the reference dose shifted by a distance proportional to the off-axis distance but along the direction perpendicular to the field edge in that quadrant. The dose was shifted by 1.2 mm cm^{-1} so that at an off-axis distance of 2.5 cm, the shift was 3 mm. Quadrant four (left quadrant) applied both dose and distance shifts. In this manner, the performance of the γ distribution to evaluate both dose and distance discrepancies in both shallow and steep dose gradient regions could be studied. The performance of the proposed geometric technique was compared against the conventional interpolation method with increasingly high grid resolutions.

Three-dimensional dosimeters are an important development in radiation therapy dosimetry.[20–22] These are typically evaluated against three-dimensional dose distribution calculations. Another three-dimensional dose comparison application is the comparison of a treatment planning system dose calculation with a calculation made using an independent system.[23] Both of these scenarios require a quantitative comparison tool and the γ tool will be a useful tool if it is accurately computed. The proposed method was evaluated by expanding the original two-dimensional simulated dose distribution into the depth direction by applying divergence (assuming a 100 cm source-to-surface distance) and depth-dose behavior (5% cm^{-1}). Surface buildup was not simulated. The evaluated field was created by applying a constant shift of 4 mm in each x, y, and z direction to the reference field and both distributions were $20\times20\times5$ cm^3 in size. Figure 4 shows coronal and sagittal projections through the three-dimensional dataset. The spatial resolution was $1\times1\times1$ mm^3.

III. RESULTS

Figure 5 shows the γ distributions computed by the conventional interpolation method and the proposed geometric method. Note that the result using the original evaluated dose points in (a) clearly exhibits artifacts, such as ripples, discontinuities and large γ values, at regions with steep dose gradients. To achieve a similar accuracy level as the geometric method [result shown in (f)], a grid resolution of at least 16 times finer than the original has to be used in the conventional interpolation approach [shown in (e)]. While such artifacts are reduced as the interpolation resolution increases, the computational cost also increases dramatically. Using a Core-2 duo 6600 processor, the time required to compute the two-dimensional γ test using the original, uninterpolated evaluated dose points and the geometric method were 0.34 and 0.38 s, respectively. However, when the factor-of-16 in-

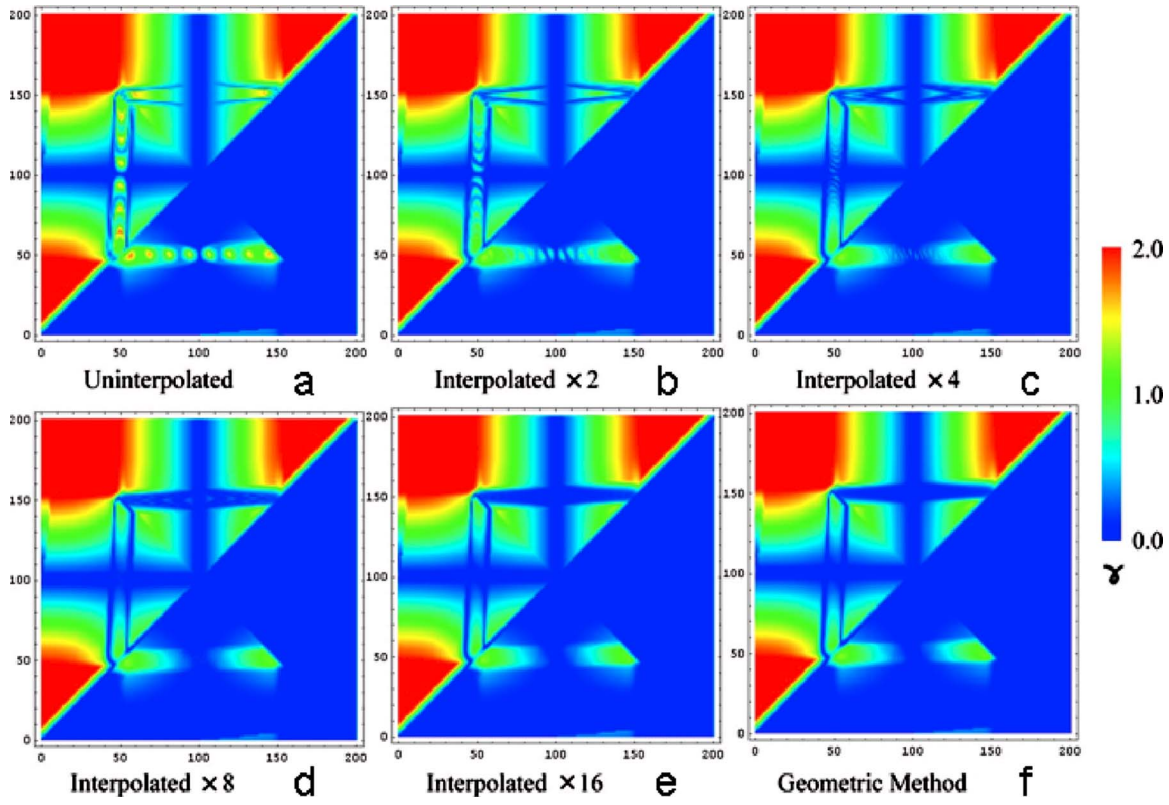

FIG. 5. Results of the two-dimensional γ distribution tests (3% and 3 mm comparison criteria). The two dose distributions shown in Fig. 3 were compared using the interpolation method (a–e) and the poposed geometric method (f). The interpolation method was conducted at increasingly high spatial resolutions that are 2, 4, 8 and 16 times finer than the original 1×1 mm^2 resolution.

terpolation was used, 9.9 s was consumed to conduct the γ calculation using the interpolation method. Therefore, in order to get accurate γ distributions, the geometric calculation provided a much more efficient computation method.

While the times required to calculate γ in two dimensions were relatively small, the time required for three dimensions was notably longer. The γ distributions computed using the original evaluated dose points (without interpolation) and using our geometric method are shown in Fig. 6. Both distributions are computed within minutes, requiring 67 and 127 s, respectively. However, without interpolation or using the geometric computation, larger errors of γ appear where dose gradients are steeper, as shown in (a) (the periodic wave behavior exhibited in Fig. 5 is not apparent because the penumbra are parallel in Fig. 6). To achieve a similar level of accuracy as the geometric method, the conventional interpolation approach would require a finer grid resolution than the original, which would result in a cubically growing calculation time[19] that far exceeds that of the proposed geometric method.

IV. CONCLUSIONS

An accurate and efficient method for computing the γ function for comparing two-dimensional and three-dimensional dose distributions has been proposed. The new method utilizes a geometric representation of the dose distribution, and produces accurate results independent of dose gradients and grid spacing. As demonstrated in the test examples, at equivalent γ calculation accuracy, the proposed method is much more efficient than the traditional interpolation method. In general, the γ values computed by interpolation have artifacts in steep dose gradient regions that cause an overestimation of γ. This is because the Euclidean distance from a reference position to the evaluated dose surface is a lower bound of the distance between the reference position and any sampled point on that surface. Using the simplicial mesh representation of the dose surface, the proposed method of calculating γ is as accurate as linear interpolation within each simplex but much more efficient relative to interpolation.

The use of the geometric model for the calculation of γ does not preclude the need for an exhaustive search. The distance between each simplex and the reference dose point requires calculation so that the minimum value can be determined. The search can be limited according to the DTA criterion based on the maximum value of γ that the user needs to quantitatively compute. For example, if the maximum value of γ for which the user requires a quantitative determination is $\gamma=10$, the maximum radial distance required for the γ search is ten times the DTA criterion.

The geometric computation of γ also allows the use of a lower-resolution grid for dose comparison in place of the original high-resolution does distributions. Since the geometric method is as accurate as linear interpolation, the γ com-

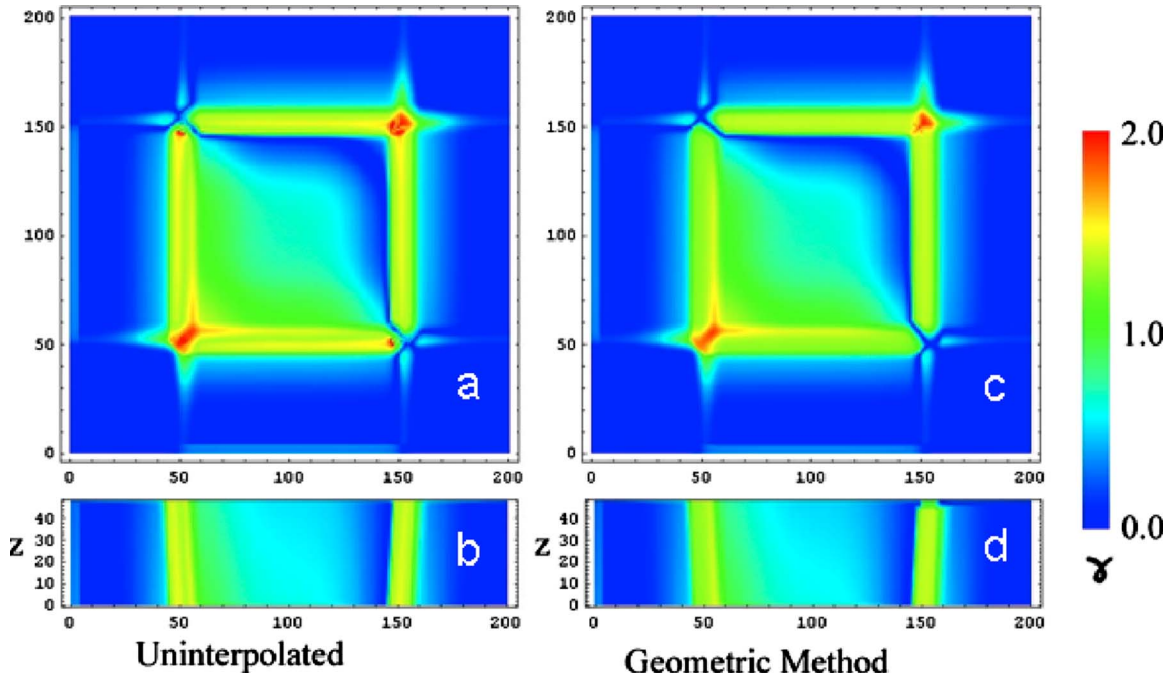

FIG. 6. Three-dimensional γ distribution computed by using the original evaluated dose points (left, without interpolation) and using the proposed geometric method (right).

puted at a lower resolution (e.g., 2 mm) would be accurate compared to that computed at a higher resolution (e.g., 1 mm) in regions where the higher-resolution distribution exhibits a linear behavior, that is, where the second derivative (e.g., change in the gradient) of the dose is small.

This computational tool has been integrated into the open-source Computational Environment for Radiotherapy Research,[24] and will be made available in a future release of that system.

ACKNOWLEDGMENTS

This work is supported in part by Grant Nos. NIH CA096679 and NIH R01 CA85181.

[a]Author to whom correspondence should be addressed. Electronic mail: taoju@cs.wustl.edu

[1]D. A. Low and J. F. Dempsey, "Evaluation of the gamma dose distribution comparison method," Med. Phys. **30**, 2455–2464 (2003).
[2]W. B. Harms, D. A. Low, J. W. Wong, and J. A. Purdy, "A software tool for the quantitative evaluation of 3D dose calculation algorithms," Med. Phys. **25**, 1830–1836 (1998).
[3]J. Van Dyk, R. B. Barnett, J. E. Cygler, and P. C. Shragge, "Commissioning and quality assurance of treatment planning computers," Int. J. Radiat. Oncol., Biol., Phys. **26**, 261–273 (1993).
[4]A. Cheng, W. B. Harms, R. L. Gerber, J. W. Wong, and J. A. Purdy, "Systematic verification of a three-dimensional electron beam dose calculation algorithm," Med. Phys. **23**, 685–693 (1996).
[5]D. A. Low, W. B. Harms, S. Mutic, and J. A. Purdy, "A technique for the quantitative evaluation of dose distributions," Med. Phys. **25**, 656–661 (1998).
[6]A. L. Boyer, E. B. Butler, T. A. DiPetrillo, M. J. Engler, B. Fraass, W. Grant, C. C. Ling, D. A. Low, T. R. Mackie, R. Mohan, J. A. Purdy, M. Roach, J. G. Rosenman, L. J. Verhey, J. W. Wong, R. L. Cumberlin, H. Stone, and J. R. Palta, "Intensity-modulated radiotherapy: Current status and issues of interest," Int. J. Radiat. Oncol., Biol., Phys. **51**, 880–914 (2001).
[7]B. Caccia, C. Andenna, C. Zicari, and S. Marzi, "Comparison of dose distributions in IMRT planning using gamma factor: Some clinical cases," Radiother. Oncol. **73**, S331–S331 (2004).
[8]G. Cernica, S. F. de Boer, A. Diaz, R. A. Fenstermaker, and M. B. Podgorsak, "Dosimetric accuracy of a staged radiosurgery treatment," Phys. Med. Biol. **50**, 1991–2002 (2005).
[9]S. Cilla, P. Viola, L. Azario, L. Grimaldi, M. Craus, G. D'Onofrio, A. Fidanzio, F. Deodato, G. Macchia, C. Digesu, A. G. Morganti, and A. Piermattei, "Comparison of measured and computed portal dose for IMRT treatment," J. Appl. Clin. Med. Phys. **7**, 65–79 (2006).
[10]P. Kipouros, P. Papagiannis, L. Sakelliou, P. Karaiskos, P. Sandilos, P. Baras, I. Seimenis, M. Kozicki, G. Anagnostopoulos, and D. Baltas, "3D dose verification in Ir-192 HDR prostate monotherapy using polymer gels and MRI," Med. Phys. **30**, 2031–2039 (2003).
[11]A. F. Monti and G. Frigerio, "Dosimetric verification of 6 and 18 MV intensity modulated photon beams using a dedicated fluoroscopic electronic portal imaging device (EPID)," Radiother. Oncol. **81**, 88–96 (2006).
[12]M. P. Petric, B. G. Clark, and J. L. Robar, "A comparison of two commercial treatment-planning systems for IMRT," J. Appl. Clin. Med. Phys. **6**, 63–80 (2005).
[13]W. D. Renner, "3d dose reconstruction to insure correct external beam treatment of patients," Med. Dosim. **32**, 157–165 (2007).
[14]S. Vedam, A. Docef, M. Fix, M. Murphy, and P. Keall, "Dosimetric impact of geometric errors due to respiratory motion prediction on dynamic multileaf collimator-based four-dimensional radiation delivery," Med. Phys. **32**, 1607–1620 (2005).
[15]M. Wendling, R. J. W. Louwe, L. N. McDermott, J. J. Sonke, M. van Herk, and B. J. Mijnheer, "Accurate two-dimensional IMRT verification using a back-projection EPID dosimetry method," Med. Phys. **33**, 259–273 (2006).
[16]M. Stock, B. Kroupa, and D. Georg, "Interpretation and evaluation of the gamma index and the gamma index angle for the verification of IMRT hybrid plans," Phys. Med. Biol. **50**, 399–411 (2005).
[17]A. Bakai, M. Alber, and F. Nusslin, "A revision of the gamma-evaluation concept for the comparison of dose distributions," Phys. Med. Biol. **48**, 3543–3553 (2003).
[18]T. Depuydt, A. Van Esch, and D. P. Huyskens, "A quantitative evaluation of IMRT dose distributions: Refinement and clinical assessment of the gamma evaluation," Radiother. Oncol. **62**, 309–319 (2002).
[19]M. Wendling, L. J. Zijp, L. N. McDermott, E. J. Smit, J. J. Sonke, B. J. Mijnheer, and M. Van Herk, "A fast algorithm for gamma evaluation in

3D," Med. Phys. **34**, 1647–1654 (2007).
[20]C. Boudou, I. Tropres, J. Rousseau, L. Lamalle, J. F. Adam, F. Esteve, and H. Elleaume, "Polymer gel dosimetry for synchrotron stereotactic radiotherapy and iodine dose-enhancement measurements," Phys. Med. Biol. **52**, 4881–4892 (2007).
[21]R. A. Crescenti, S. G. Scheib, U. Schneider, and S. Gianolini, "Introducing gel dosimetry in a clinical environment: Customization of polymer gel composition and magnetic resonance imaging parameters used for 3D dose verifications in radiosurgery and intensity modulated radiotherapy," Med. Phys. **34**, 1286–1297 (2007).
[22]H. Gustavsson, A. Karlsson, S. A. J. Back, L. E. Olsson, P. Haraldsson, P. Engstrom, and H. Nystrom, "MAGIC-type polymer gel for three-dimensional dosimetry: Intensity-modulated radiation therapy verification," Med. Phys. **30**, 1264–1271 (2003).
[23]W. Luo, J. Li, R. A. Price, Jr., L. Chen, J. Yang, J. Fan, Z. Chen, S. McNeeley, X. Xu, and C. M. Ma, "Monte Carlo based IMRT dose verification using MLC log files and R/V outputs," Med. Phys. **33**, 2557–2564 (2006).
[24]J. O. Deasy, A. I. Blanco, and V. H. Clark, "CERR: A computational environment for radiotherapy research," Med. Phys. **30**, 979–985 (2003).